6th World Congresses of Structural and Multidisciplinary Optimization
Rio de Janeiro, 30 May - 03 June 2005, Brazil

A checkerboard-controlling filter for topology optimization based on stress distribution

Kazem Ghabraie, Soheil Mohammadi

Department of Civil Engineering, Faculty of Engineering, University of Tehran, Tehran, Iran
Email: kazem.ghabraie@gmail.com, smoham@ut.ac.ir

Abstract: The checkerboard patches are known as one of major instabilities in topology optimization algorithms that should be overcame in order to sure the manufacturability of the final topology. In this paper the relationship between stress/strain distribution and checkerboard formation is investigated and with some examples it is illustrated that smoother stress/strain distributions result in topologies with fewer checkerboards. Based on this fact, a checkerboard controlling filter is introduced. This new approach dose not restricts the design domain and no direct modification is applied to design variables or sensitivities. In this approach the only revision is smoothing stress/strain distributions. Different numerical examples are solved using this approach and all results were free from checkerboards. The results showed that the approach may also overcome the local minima problem which is another common instability in topology optimization problems. A detailed comparison between the new approach and a known checkerboard controlling filter is made.
Keywords: topology optimization, checkerboard, stress distribution, controlling filters, SIMP method

1. Introduction

Finding the best topology of structural layout or Topology Optimization is of great importance in design process, and a great amount of work has been done in this area during the last decade. In structural topology optimization problems, material distribution methods are very common due to their precise and simple definition of the problem and their satisfactory results. In these methods topology is represented by material distribution in the design domain of the problem. By modifying material properties one can model different topologies in these methods and hence there is no need for remeshing. Using Solid Isotropic Material with Penalization or SIMP method is one of the material distribution methods, which is frequently used in structural topology optimization. In this method, which is to be considered in this paper, the element relative densities are considered as design variables. Within each element, the material properties are assumed constant and are described by the so-called power-low interpolation [1, 2, 3]. Design variables (element relative densities) vary continuously between 0 (void) and 1 (solid). The power-law interpolation penalizes the intermediate densities and pressurizes them into boundary values. The topology obtained here is represented by a grey scale image which consists of solid (black) elements, void (white) elements and elements with intermediate densities (grey elements).

The SIMP method, like the other material distribution methods, suffers from numerical instabilities such as checkerboards, mesh-dependency and local minima [4]. In this paper we deal with the checkerboard problem which refers to the formation of areas of alternating solid and void elements in a checkerboard-like pattern. It is demonstrated by Diaz and Sigmund (1995) that these patches may generate unrealistic high stiffness in displacement based finite element analysis (see [5]) while the reason is not quite known. In this study the relationships between stress/strain distribution and checkerboard formation are investigated. This investigation might be found useful in finding the source of this instability.

In the literature there are some known approaches that can overcome the checkerboard problem [6]. These approaches could be classified into three categories. The first category, sometimes referred to as Restriction methods, consists of those approaches that restrict the design space by introducing additional constraints for example on perimeter or density slopes (see [7], [8]). There is another class of approaches in which design variables or sensitivities are modified in order to remove the checkerboard pattern. These methods are usually referred to as Filtering approaches and are more widely used with SIMP method [3]. Finally one may use special types of finite elements to overcome the instability. Higher order finite elements as well as non-conforming finite elements could be used here. Although higher order finite elements do not completely resolve the checkerboard problem [5], using non-conforming finite elements, as reported by Jang et al. (2000), could overcome this instability completely [9].

In this paper, it is shown that checkerboard formation is influenced by stress/strain distributions and smoothing stress/strain distributions in finite elements may remove checkerboard patches completely. Based on this result, a simple algorithm for suppressing checkerboard patches is introduced. This approach dose not restricts the design domain and doesn't need special finite elements. Besides, no direct modification is applied to design variables or sensitivities. In this approach only modification is smoothing stress/strain distributions and hence it can be regarded as a filtering approach. During verification tests, this approach did not show any kind of checkerboard instabilities and besides, some tests showed that local minima problem is overcame as well.

An overview of the paper is as follows. In section 2, through some examples relationships between checkerboard formation and stress/strain distributions are demonstrated. In section 3, we define our filtered version of the well-known minimum compliance topology optimization problem and a simple algorithm for smoothing stress/strain distribution is introduced. Some of the well-known problems in structural topology optimization are solved using this new approach and results are reported for verification in section 4. A comparison between the present approach and Sigmund's sensitivity filter [3] is made in section 5 and finally in section 6, the findings are summarized and a conclusion is made.

2. Influences of checkerboard formation and stress distribution on each other

In topology optimization problems, one may easily find some relationships between stress/strain distribution and formation of checkerboard patches. In the following some examples are given on this issue.

As the first experiment we investigate the stress distribution of a checkerboard patch to find the influence of these patches on stress distribution. To do this a same problem (MBB problem, see fig 5-a) is solved once using normal SIMP method with no controlling

technique and once using a sensitivity filter to overcome checkerboards. Optimum topologies are illustrated in fig. 1-a and 1-b and stress distributions of these topologies are depicted in fig 1-c and 1-d respectively. It should be noted that in fig 1-c and 1-d, absolute values of stresses are depicted. It could be seen that in the left solution, stresses fluctuate considerably within checkerboard patches (fig 1-c) while stress distribution of the right solution is not oscillating (fig 1-d). The reason is that solid elements (black elements) have higher stiffness in contrast to void (white) elements and so solid elements bear much more stress than void elements.

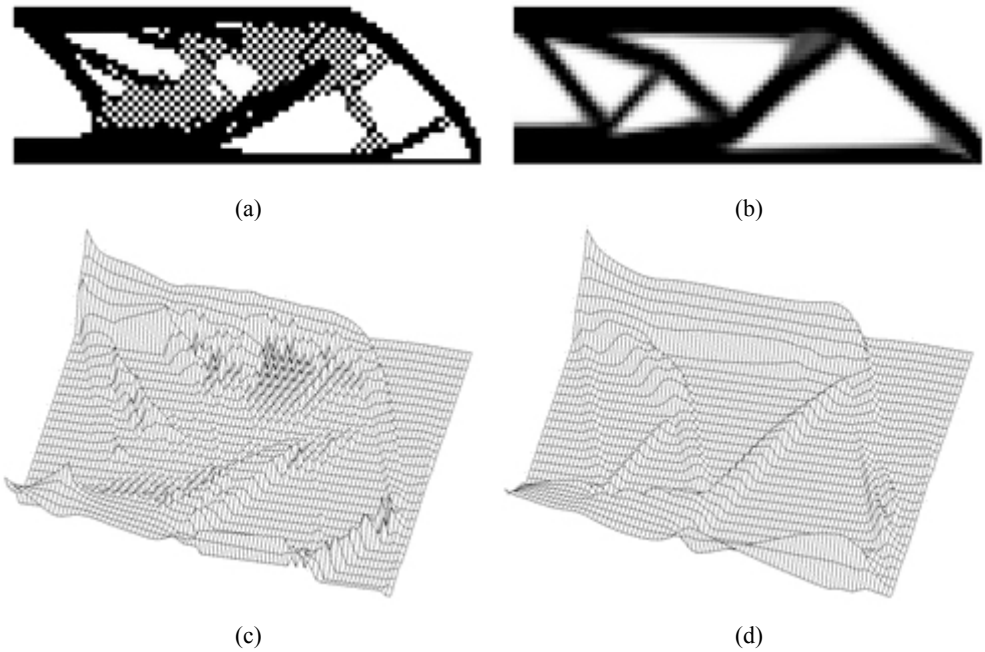

(a) (b)

(c) (d)

Figure 1. Topologies obtained by normal SIMP method without any instability control (a) and by using sensitivity filter (b) stress distributions of optimum solutions (c), (d)

At the next step, the influence of stress distribution on forming checkerboard patches is investigated. It is known that utilizing higher order finite elements which generate smoother stress/stain solutions, results in topologies with fewer or even no checkerboards [5,10]. For further study we compare solutions of two different types of finite elements namely Constant Strain Triangles (CSTs) and four-node quadrilateral finite elements. CST elements model the stress (strain) distribution by a constant stress (strain) within each element while within four-node quadrilateral elements, stress and strain distributions are assumed bilinear. Hence stress and strain distributions obtained by four-node quadrilateral elements are smoother compared to CST results. The so-called Short Cantilever Beam or SCB problem (see Fig. 4-a) is solved here using SIMP method without any modification with CST and four-node quadrilateral finite elements. Obtained topologies are illustrated in fig 6-a and 4-b respectively. It could be seen that the topology obtained through using four-node quadrilateral finite elements has less checkerboard patches in contrast to the case of CST finite elements.

Through these facts and results one may conclude two major conclusions that are (a) stresses and strains fluctuate extremely within checkerboard patches and (b) smoother stress/strain approximations result in topologies with fewer checkerboards.

Based on these results an approach for controlling checkerboard formation is introduced in the next section.

3. Statement of the problem and introducing the new approach

To investigate the influence of smoothing stress distribution on forming checkerboard patches it is necessary to reformulate the problem so that stress/strain modifications can adjust design variables. The well known compliance minimization is considered which is defined as (see [6], [3])

$$\begin{aligned} \min_{x} \quad & c(\mathbf{x}) \\ \text{subject to:} \quad & \frac{V(\mathbf{x})}{V_0} = f \\ : \quad & 0 < \mathbf{x}_{min} \leq \mathbf{x} \leq 1 \end{aligned} \tag{1}$$

where $c(\mathbf{x})$ is the mean compliance, $\mathbf{x}$ is the vector of design variables, $\mathbf{x}_{min}$ is a vector of minimum relative densities (which are considered positive to avoid singularities), $V(\mathbf{x})$ and V_0 are material and design domain volumes, respectively, and f is a prescribed value known as the volume fraction.

Mean compliance, $c(\mathbf{x})$, can be formulated in terms of stress and strain vectors as:

$$c = \int_{\Omega} \boldsymbol{\varepsilon}^T \boldsymbol{\sigma} \, \mathrm{d}\boldsymbol{\Omega} \tag{2}$$

and if the design domain $\boldsymbol{\Omega}$ is divided into N_e finite elements, we have:

$$c = \sum_{e=1}^{N_e} \int_{\mathbf{\Omega}_e} \boldsymbol{\varepsilon}_e^T \boldsymbol{\sigma}_e \, \mathrm{d}\mathbf{\Omega} \tag{3}$$

In which $\mathbf{\Omega}_e$, $\boldsymbol{\varepsilon}_e$, and $\boldsymbol{\sigma}_e$ represent volume, strain vector and stress vector of the finite element e, respectively.
For simplification a new parameter c_e is introduced as:

$$c_e = \int_{\mathbf{\Omega}_e} \boldsymbol{\varepsilon}_e^T \boldsymbol{\sigma}_e \, \mathrm{d}\mathbf{\Omega} \tag{4}$$

Using Eq.(4), Eq.(3) can be rewritten as follows:

$$c = \sum_{e=1}^{N_e} c_e \tag{5}$$

The stress vector is a function of design parameters. To show this, stress-strain relationships from the finite element method and the power-law interpolation from SIMP method are recalled [1, 6, 10]

$$\boldsymbol{\sigma}_e = \mathbf{D}_e \cdot \boldsymbol{\varepsilon}_e \ , \quad \mathbf{D}_e = x_e^p \cdot \mathbf{D}^0 \tag{6}$$

Here $\mathbf{D}^0$ is the material matrix and p is the penalization power.
By introducing the parameter $\boldsymbol{\sigma}_e^0$ as

$$\boldsymbol{\sigma}_e^0 = \mathbf{D}^0 \cdot \boldsymbol{\varepsilon}_e \tag{7}$$

and using Eq.(6) and Eq.(7) in Eq.(4) results in:

$$c_e = x_e^p \int_{\mathbf{\Omega}_e} \boldsymbol{\varepsilon}_e^T \boldsymbol{\sigma}_e^0 \, \mathrm{d}\mathbf{\Omega} \tag{8}$$

To make use of the optimality criteria technique and the heuristic updating scheme [6, 3], it is also necessary to reformulate the sensitivity of the objective function in terms of stress and strain vectors which leads to:

$$\frac{\partial c}{\partial x_e} = \frac{\partial c_e}{\partial x_e} = p \cdot x_e^{p-1} \int_{\mathbf{\Omega}_e} \boldsymbol{\varepsilon}_e^T \boldsymbol{\sigma}_e^0 \, \mathrm{d}\mathbf{\Omega} \tag{9}$$

or simply:

$$\frac{\partial c}{\partial x_e} = \frac{p \cdot c_e}{x_e} \tag{10}$$

Now if the stress and strain vectors were modified through a smoothing algorithm, the modified compliance within each element can be found as:

$$\hat{c}_e = \int_{\mathbf{\Omega}_e} \hat{\boldsymbol{\varepsilon}}_e^T \hat{\boldsymbol{\sigma}}_e \, \mathrm{d}\mathbf{\Omega} \tag{11}$$

in which $\hat{\boldsymbol{\varepsilon}}_e$ and $\hat{\boldsymbol{\sigma}}_e$ are smoothed strain and stress vectors respectively. Using Eq.(11) in Eq.(10), new sensitivities can be calculated as follows:

$$\frac{\widehat{\partial c}}{\partial x_e} = \frac{p \cdot \hat{c}_e}{x_e} \tag{12}$$

In the new statement of the problem, equations Eq.(4) and Eq.(9) are replaced by equations Eq.(11) and Eq.(12), respectively.

3.1. Smoothing algorithm

In the following, a new approach for smoothing stress/strain distribution is introduced. It should be noted that although this smoothing approach is not the only one which can eliminate checkerboards.
For each node of each finite element, all connected elements are considered. The nodal stress (strain) of each specified node is then calculated through averaging stresses (strains) of that node within each connected element.
As an example, a 3x3 mesh of 4-node quadrilateral finite elements is considered (fig 2). Within each element, nodes are numbered in a counterclockwise order as depicted in fig 2. The stress (strain) vector at node j, within element k, is represented by s^k_j. Using the described algorithm, modified stress (strain) vectors for three sample nodes which are marked in fig 2, are calculated as follows:

$$\begin{aligned} s_3^{a*} &= s_3^a, \\ s_2^{f*} &= \tfrac{1}{2}\left(s_2^f + s_1^c\right) = s_1^{c*}, \\ s_4^{e*} &= \tfrac{1}{4}\left(s_4^e + s_3^h + s_2^g + s_1^d\right) = s_3^{h*} = s_2^{g*} = s_1^{d*} \end{aligned} \tag{13}$$

In order to calculate the integral in Eq.(11) for elements with constant or linear stress/strain distribution (like CST and 4-node quadrilateral elements), it is sufficient to determine the integrand at the center of specified element multiplied by the element's volume. For bilinear stress/strain distributions (also valid for constant stress/strain distributions), the stress (strain) vector at the

centre of each element can be computed by averaging nodal stresses (strains):

$$s_c^i = \frac{1}{4}\left(s_1^i + s_2^i + s_3^i + s_4^i\right) \tag{14}$$

In this paper, this approach is used in combination with SIMP method. The approach is applied to smooth stresses and strains after each finite element analysis and the smoothed solutions are then used in Eq.(11) and Eq.(12) to calculate adjusted sensitivities. The flow of this procedure is depicted in fig 3.

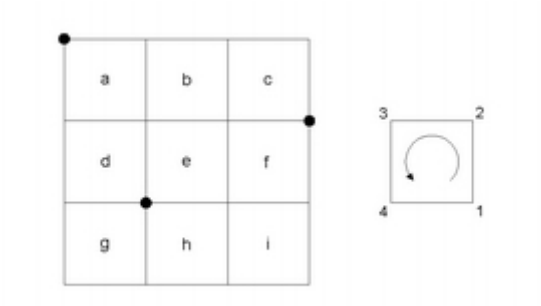

Figure 2. An example of a mesh of 9 four-node quadrilateral elements

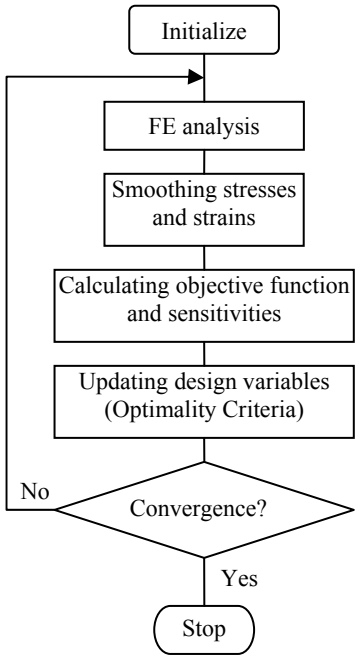

Figure 3. Algorithm of the new approach

4. Numerical examples

To verify the present approach five examples are considered. In the first two examples as well as in the last two ones, uniform mesh of four-node quadrilateral square elements is used while an unstructured mesh of CST elements is used in the third example. Through the first three examples it is demonstrated that this approach could overcome the checkerboard problem and the fourth example illustrates that this approach could relieve the local minima instability. The last example deals with mesh-dependence instability. This example shows that this approach could not overcome mesh-dependency.

In all of these examples the following parameters are adopted: modulus of elasticity E=1.0, Poisson's ratio ν=0.3 and applied force F=1.0. All units are assumed to be consistent. The power-law approach with the exponent p=3 is used here and the material volume is restricted to one half of the design volume (f=0.5).

4.1. Structured mesh with quadrilateral finite elements

In the following examples a uniform mesh of four-node quadrilateral square finite elements is used. All elements are equal in size. The first example is the well-known short cantilever beam (SCB) problem with a mesh of 90 x 60 elements. The left side of the beam is fixed and a downward concentrated force is applied at the middle of the right side. The design domain of this problem is shown in fig 4-a. The final topologies obtained by normal SIMP method and the new approach are illustrated in fig 4-b and 4-c respectively.

The second example is the MBB beam problem whose design domain is depicted in fig 5-a. Half of the design domain with symmetry conditions is modeled here (fig 5-b). A 90 x 30 mesh is used for this modeling. Figures 1-a and 5-c illustrate the topologies obtained using normal SIMP method and the new approach respectively. It could be seen that in both cases using smoothed

stress/strain distribution removes the checkerboard pattern.

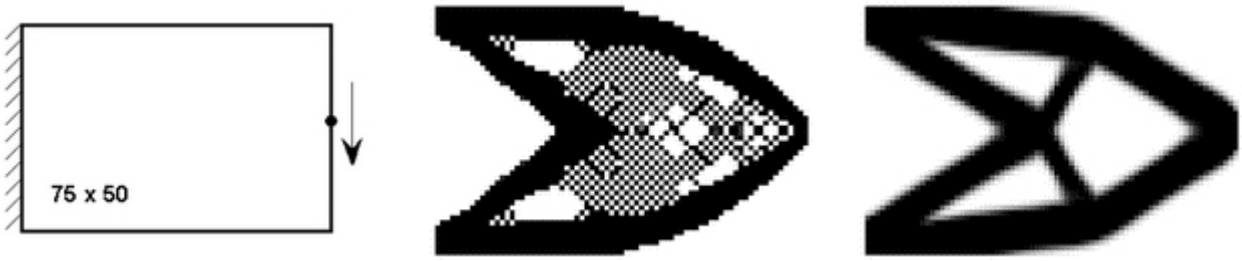

(a) (b) (c)

Figure 4. Short Cantilever Beam problem - design domain (a) and optimum topologies obtained by normal SIMP method (b) and by the new approach (c)

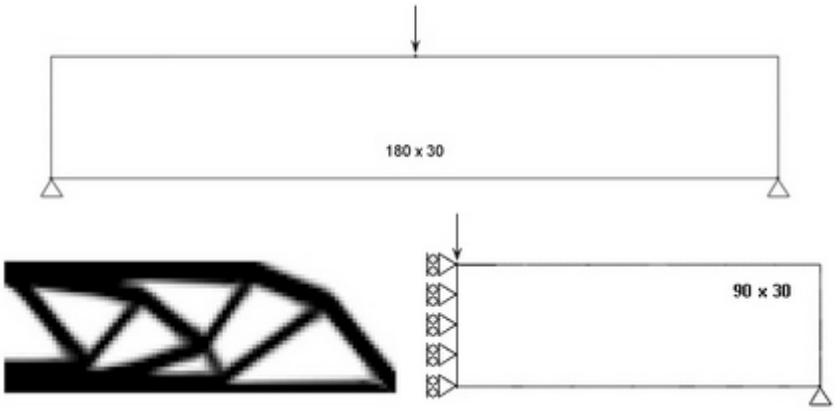

(c) (b)

Figure 5. MMB Beam problem - design domain (a), half design domain with symmetry conditions (b), and optimum solution obtained by the new approach (c)

4.2. Unstructured mesh with CST finite elements

This example is the same SCB problem which was solved in the first example (fig 4-a) except the mesh used here is an unstructured mesh of 3776 CST elements. Obtained topologies are shown in fig 6-a and 6-b. The topology obtained by the new approach in both cases is free from checkerboards and qualitatively remains unchanged (see fig 6-b and 4-c). This demonstrates that functioning of this new approach is independent of the type of mesh and elements.

(a) (b)

Figure 6. Using unstructured mesh of CST elements - optimum topologies obtained by normal SIMP method (a) and by the new approach (b)

4.3. Local minima and mesh-dependency

Through the following examples we seek if the present approach could relieve local minima and mesh-dependence instabilities as well. The mesh-dependence problem refers to obtaining different topologies for different mesh parameters while the problem of obtaining different solutions for the same mesh but different algorithmic parameters referred to as local minima [4].

Again the MBB problem whose design domain is depicted in fig 5-a, is considered. To investigate the local minima problem the new approach was implemented to different initial conditions. Initial conditions are depicted in fig 7-a and 7-b and the obtained topologies for each one are illustrated in fig 7-c and 7-d respectively. No qualitative difference could be found in these solutions.

In the next example different mesh sizes with 60x20 and 120x40 quadrilateral elements are considered for the same MMB problem. Obtained solutions are illustrated in fig 8-a and 8-b respectively. It could be seen that using finer meshes results in introduction of more holes in the optimum solution. To describe the reason, Bendsøe and Sigmund (2004) stated that “the introduction of more

holes, without changing the structural volume, will generally increase the efficiency of a given structure" (see [6]). It is clear that the obtained topologies are mesh-dependent and the new approach could not overcome the mesh-dependency. However it should be noted here that whilst mesh-independent solutions are necessary for obtaining practical simple topologies, as correctly noted by Rozvany (2001), "mesh-dependence actually becomes beneficial if we want to demonstrate that topologies tend to a known exact solution" [11].

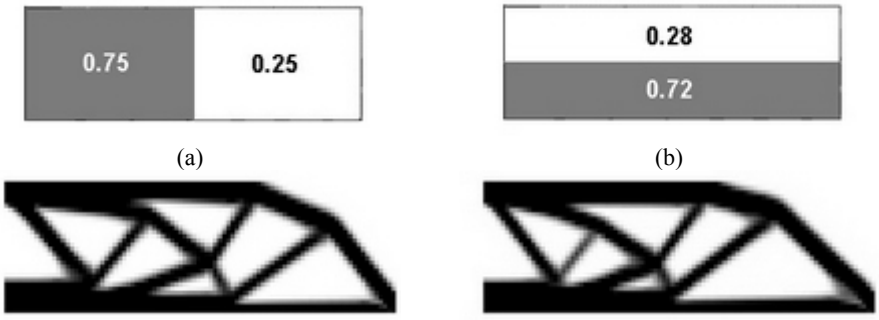

(a) (b)

(c) (d)

Figure 7. Local minima - topology optimization of MMB beam problem: different initial density distributions (a), (b) and optimum solutions obtained by the present approach (c), (d)

(a) (b)

Figure 8. Mesh-dependency - optimum topologies of MMB problem using 60x20 (a) and 120x40 (b) mesh sizes

5. Comparison

In this section the present approach is compared with Sigmund's sensitivity filter which is a known checkerboard controlling technique. In Sigmund's sensitivity filter (SSF) the calculated sensitivities (Eq.(9)) are replaced by

$$\widehat{\frac{\partial c}{\partial x_e}} = \frac{1}{x_e \sum_{f=1}^{N_e} \hat{H}_f} \sum_{f=1}^{N_e} \left(\hat{H}_f x_f \frac{\partial c}{\partial x_f} \right) \tag{15}$$

In which $\hat{H}_f$ is a weight factor written as

$$\begin{aligned} &\hat{H}_f = max\{0,\ r - \mathrm{dist}(e,f)\}, \\ &(e,f) \in \mathrm{N} \times \mathrm{N}, \quad \mathrm{N} = \{1,\ldots,N_e\}. \end{aligned} \tag{16}$$

Where dist(*e*,*f*) is defined as the distance between centre of element *e* and centre of element *f* and *r* is a parameter that defines the radius of the filtered area (see [3]).

It could be seen that in SSF, sensitivity of each element is modified with respect to sensitivities of neighboring elements and the filter works similar to filters used in image processing. If within each element stresses and strains assumed constant, modified sensitivities obtained by the new approach and SSF will be somehow similar to each other as they both normalize element sensitivity with respect to sensitivities within neighboring elements. For more explanation we rewrite Eq.(15) using Eq.(10).

$$\widehat{\frac{\partial c}{\partial x_e}} = \frac{1}{x_e \sum_{f=1}^{N_e} \hat{H}_f} \sum_{f=1}^{N_e} \left(\hat{H}_f p c_f \right) \tag{17}$$

Noting that *p* is constant for all elements and using Eq.(12) in Eq.(17) we have

$$\frac{p \cdot \hat{c}_e}{x_e} = \frac{p \sum_{f=1}^{N_e} \hat{H}_f c_f}{x_e \sum_{f=1}^{N_e} \hat{H}_f} \tag{18}$$

or simply

$$\hat{c}_e = \frac{\sum_{f=1}^{N_e} \hat{H}_f c_f}{\sum_{f=1}^{N_e} \hat{H}_f} \tag{19}$$

As stress and strain vectors within each element are assumed constant, the element compliance c_e (see Eq.(4)) could be found through following

$$c_e = \boldsymbol{\varepsilon}_e^T \boldsymbol{\sigma}_e V_e \tag{20}$$

where Ve denotes volume of element e. Finally using Eq.(20) in Eq.(19) the following equation is derived for SSF

$$\boxed{\hat{c}_e = \frac{\sum_{f=1}^{N_e} \hat{H}_f \boldsymbol{\varepsilon}_f^T \boldsymbol{\sigma}_f V_f}{\sum_{f=1}^{N_e} \hat{H}_f}} \tag{21}$$

A similar equation could be found for the new approach. The element modified compliance $\hat{c}_e$ (see Eq.(11)) can be written as

$$\hat{c}_e = \hat{\boldsymbol{\varepsilon}}_e^T \hat{\boldsymbol{\sigma}}_e V_e \tag{22}$$

Using the smoothing algorithm described in section 3, smoothed stress and strain vectors at the centre of element *e* can be described by

$$\hat{\boldsymbol{\varepsilon}}_e = \frac{\sum_{f\in \mathrm{F}_e} \hat{W}_f \boldsymbol{\varepsilon}_f}{\sum_{f\in \mathrm{F}_e} \hat{W}_f}, \quad \hat{\boldsymbol{\sigma}}_e = \frac{\sum_{f\in \mathrm{F}_e} \hat{W}_f \boldsymbol{\sigma}_f}{\sum_{f\in \mathrm{F}_e} \hat{W}_f} \tag{23}$$

In Eq.(23) $\hat{W}_f$ is a weight factor which can be calculated using smoothing algorithm and F_e denotes elements connected to element *e*. Using Eq.(23) in Eq.(22) the following equation could be derived for the new approach

$$\boxed{\hat{c}_e = \frac{\left(\sum_{f\in F_e} \hat{W}_f \boldsymbol{\varepsilon}_f^T\right)\left(\sum_{f\in F_e} \hat{W}_f \boldsymbol{\sigma}_f\right)}{\left(\sum_{f\in F_e} \hat{W}_f\right)^2} V_e} \tag{24}$$

It should be noted that the Eq.(24) which is derived for the new approach is based on the assumption of constant stress and strain states within elements. This assumption is not valid for many cases (such as four-node quadrilateral or higher order finite elements) and in these cases this equation would be more complicated. In this comparison, however, we use Eq.(24) because of its simplicity and its similarity with Eq.(21).

It is clear that both approaches find filtered element compliance (and subsequently element sensitivity) through averaging stresses and strains within neighboring elements. However while the new approach normalizes stress and strain vectors separately, in SSF their scalar product is normalized. The other obvious difference is about the influence of volumes of neighboring elements in each technique. In Eq.(21) (SSF) the filtered parameters of each element are directly influenced by volumes of neighboring elements while in the new approach the filtered element compliance (and subsequently element sensitivity) within each element only depends on volume of that element itself. In uniform structured meshes like those used in examples 1, 2, 4 and 5, this feature is not important as all elements are of the same size. However in using SSF with non-uniform or unstructured meshes one should choose the filter's radius carefully because if sizes of some elements are greater than the chosen filter's radius, eliminating checkerboards is not assured. In these cases large element sizes, even if they are smaller than the radius of filtering area, affect filtered sensitivities of neighboring elements considerably (see Eq.(21)).

A noticeable advantage of SSF in contrast to the new approach is that in SSF, one could obtain different topologies by changing the radius of filtering area. In this technique number of holes in the final topology could be controlled by adjusting the filtering radius. As a general rule, greater filtering radii result in simpler topologies with fewer holes. This feature could be used to obtain same topologies from different mesh sizes. In the other words SSF technique could overcome the mesh-dependency problem.

6. Conclusions

In this study it has been shown that the formation of checkerboard patches in topology optimization depends on stress distribution. Filtered version of minimum compliance topology optimization problem has been derived and a simple algorithm for smoothing stress and strain distributions has been introduced. This algorithm was used in combination with the so-called SIMP method and the approach was verified by numerical examples. Verification examples have shown that this technique may relieve the local minima problem as well. Also it was demonstrated that functioning of this approach is independent of the type of mesh and elements. at the end of the paper the approach was compared with Sigmund's sensitivity filter.

7. References

1. Bendsøe M.P. Optimal shape design as a material distribution problem. Structural Optimization, 1989, 1: 193-202
2. Rozvany G.I.N. Zhou M. Birker T. and Sigmund O. Topology Optimization using Iterative Continuum-Type Optimality Criteria (COC) Methods for Discretized Systems. In: Bendsøe M.P. Mota Soares C.A. (eds.) Topology Design of Structures, Dordrecht: Kluwer Academic Publishers, 1993, 273-286
3. Sigmund O. A 99 line topology optimization code written in Matlab. Structural and Multidisciplinary Optimization, 2001, 21: 120-127
4. Sigmund O. and Petersson J. Numerical instabilities in topology optimization: A survey on procedures dealing with checkerboards, mesh-dependencies and local minima. Structural and Multidisciplinary Optimization, 1998, 16(1): 68-75
5. Díaz A. and Sigmund O. Checkerboard patterns in layout optimization, Structural Optimization, 1995, 10: 40-45
6. Bendsøe M.P. and Sigmund O. Topology Optimization – Theory, Methods and Applications, Berlin: Springer-Verlag, 2003-04
7. Haber R.B. Jog C.S. and Bendsøe M.P. A new approach to variable-topology shape design using a constraint on perimeter. Structural Optimization, 1996, 11: 1-12
8. Petersson J. and Sigmund O. Slope constrained topology optimization, International Journal for Numerical Methods in Engineering 1998, 41: 1417-1434
9. Jang G.-W. Jeong J.H. Kim Y.Y. Sheen D. Park C. and Kim M.-N. Checkerboard-free topology optimization using non-conforming finite elements, International Journal for Numerical Methods in Engineering 2003, 57: 1717-1735
10. Hassani B. and Hinton E. Homogenization and Structural Topology Optimization – Theory, Practice and Software, London: Springer-Verlag, 1999
11. Rozvany G.I.N. Aims, scope, methods, history and unified terminology of computer-aided topology optimization in structural mechanics, Structural and Multidisciplinary Optimization, 2001,21: 90-108